J Wood Sci (2015) 61:569–577
DOI 10.1007/s10086-015-1504-9

ORIGINAL ARTICLE

Analysis of the hollow structure with functionally gradient materials of moso bamboo

Lianchun Long[1] · Zhaokun Wang[1] · Kai Chen[1]

Received: 7 April 2015 / Accepted: 4 August 2015 / Published online: 30 August 2015

Abstract Bamboo is a fiber-reinforced bio-composite with superior structural behavior. The hollow structure as well as the gradient distribution of bamboo fiber is the embodiment of the superior bamboo construction. To validate this, tensile tests were performed on bamboo test specimens. The volume fractions of bamboo fiber and parenchymatous ground tissue along the radius of the culm wall were scanned and calculated. The elastic moduli of bamboo fiber and parenchymatous ground tissue were estimated, according to the linear equations obtained by regression analysis. With the equivalent volume, a numerical hollow model and solid model were built to make comparative analysis on their mechanical behavior. For the purpose of verifying the advantage of fiber gradient distribution, models, which were composed of fiber and parenchymatous ground tissue with different fiber distributions, were built for comparative analysis. Results show that under the condition of using the same material, the hollow structure as well as fiber gradient distribution of bamboo possess excellent mechanical performance of bamboo structure.

Keywords Moso bamboo · Tensile test · Hollow structure · Gradient distribution

✉ Lianchun Long
longlc@bjut.edu.cn

[1] College of Mechanical Engineering and Applied Electronics Technology, Beijing University of Technology, No.100, Pingleyuan, Chaoyang District, 100124 Beijing, China

Introduction

Moso bamboo is a common renewable structural material with excellent mechanical performance. The structure of moso bamboo is unique and perfect, which the conical and hollow structure with diameter and culm-wall thickness that decreases along the height direction. When the total amount of the material as well as the height is constant, the structure will have obvious advantages in bearing loads compared with other structures.

At present, many studies focus on mechanical properties of bamboo. Ahmad et al. [1] have studied the physical and mechanical characteristics of Calcutta bamboo with respect to location along the length of the bamboo culm, nodes versus internodes section, and radial versus tangential directions. Low et al. [2] have investigated the microstructure, mechanical, impact, and fracture properties of Australian bamboo. Hankun Wang et al. [3] established and validated a two-variable model for predicting the combined effects of moisture content and specific density on compressive strength parallel to the grain for moso bamboo. Amada et al. [4] have reported on the fracture toughness of bamboo culms and nodes. It was concluded in the paper that the fracture toughness of the bamboo culm depends on the volume fraction of fibers. Obataya et al. [5] have compared the bending properties of split bamboo culm with those of spruce and beech wood specimens. Verma et al. [6] have analyzed the tensile properties of bamboo laminae, which were prepared from bamboo slivers, and were selected from different regions of bamboo culms (*Dendrocalamus strictus*). Yu et al. [7] have measured the mechanical properties of single bamboo fibers, extracted from 11 commercial bamboo species with a microtensile technique to understand bamboo fibers' reinforcing potential. Gutu [8] carried out the experiments on

the strength properties of bamboo, including tensile, compressive, bending, stiffness, elasticity, hardness, and durability of bamboo, in order to resist different forces or loads on structural members. Liu et al. [9] pointed that bamboo fibers possess versatile advantages of easy accessibility, high aspect ratio, and strength-to-weight ratio, which make the ideal potential replacements for manmade fibers.

The bamboo culm wall is mainly composed of bamboo fibers and parenchymatous ground tissue. An increasing distribution density of bamboo fibers exists from the inner to the outer part of the culm wall along the radial direction. Thus, the macro-mechanical properties of bamboo are variable along the same direction. Ghavami et al. [10] have made meso-structure analyses of bamboo culms through Digital Image Analysis and established the variation of the volume fraction of the cellulose fibers across the transversal section of the bamboo. Tommy et al. [11] have concluded that the fiber density of sclerenchyma tissue within the bamboo is a good indicator of the strength capacity of bamboo. Ray et al. [12] pointed out that bamboo is one of the best functionally gradient composite materials available, with the fibers that vary from outer to inner-most periphery, and the structural behavior causes the variation of tensile strength. Hankun Wang et al. [13] determined longitudinal tensile modulus, ultimate tensile strength and elongation at break of single bamboo fibers aged 0.5, 1.5 and 2.5 years old for four different moisture content levels thinking that the mechanical response of bamboo fibers to variation in moisture content has a direct influence on the performance of bamboo fiber-based products. Shao et al. [14] have analyzed the mechanical properties of bamboo as a function of its components; they also have estimated the tensile strength, modulus of elasticity (MOE) of bamboo fiber, and parenchymatous tissue.

Most work in the literature that characterizes bamboo is experimental, and dedicated to estimating strength and stiffness properties. However, very little work, which treats the modeling of natural fibers, has been found in the literature. Silva et al. [15] have investigated the structural behavior of bamboo by using finite-element method and homogenization methods. Three-dimensional models of bamboo were built and simulated under tension, torsion, and bending load cases. Tan et al. [16] studied the local variations in the Young's moduli of moso culm bamboo cross-sections by using nanoindentation techniques. Then, these are incorporated into finite-element models in which the actual variations in Young's moduli are used to model the deformation of bamboo during fracture toughness experiments, and to predict the toughening observed during resistance curve tests.

Although bamboo is now a well-established area of interest, there is still a dearth of knowledge relating to treating the modeling of natural fibers using numerical methods. Most scholars dedicate to estimating strength and stiffness properties experimentally, there is still very little study on the bamboo about verifying the advantage of bamboo construction numerically. Hence, this work will address this issue by building models composed of fiber and parenchymatous ground tissue with different fiber distributions for the purpose of verifying the advantage of fiber gradient distribution on the basis of the experimental data.

In this study, tensile tests were performed on bamboo test specimens. The volume fractions of bamboo fiber and parenchymatous ground tissue along the radius of the culm wall were measured and calculated. The elastic moduli of bamboo fiber and parenchymatous ground tissue were estimated according to the linear equations obtained by regression analysis. A numerical hollow model and a numerical solid model with the equivalent volume were built to make comparative analysis on their mechanical behavior. Models composed of fiber and parenchymatous ground tissue were built to verifying the advantage of bamboo construction, which were based on real distribution to analyze the effects of fiber gradient distributions on bamboo structural behavior.

Experimental theory

Bamboo is a fiber-reinforced bio-composite whose culm wall is mainly composed of bamboo fiber and parenchymatous ground tissue. Bamboo fibers have high strength and MOE, while parenchymatous ground tissue has low strength and MOE. In view of mechanical behavior, the bamboo block can be simplified as a composite of parallel connection model, which is composed of fibers and parenchymatous ground tissue. σ, $\sigma_{f,}$ σ_p were noted as the tensile stress of the bamboo specimen, fiber and parenchymatous ground tissue, respectively. ε, E and A were the corresponding strain, MOE, and area on the transverse section of the bamboo specimen. The volume fractions of bamboo fiber V_f and parenchymatous ground tissue V_p can be calculated as $V_f = A_f/A$ and $V_p = A_p/A$, respectively. It is also obvious that $V_f + V_p = 1$ is tenable. When the specimen bears external forces, according to the parallel connection model, the fibers and parenchymatous ground tissue should share the loads, and their strains are equal. Therefore, the following equations can be deduced:

$$\sigma = \sigma_f V_f + \sigma_p V_p = \sigma_f V_f + \sigma_p (1 - V_f) \quad (1)$$

$$E = E_f V_f + E_p V_p = E_f V_f + E_p (1 - V_f) \quad (2)$$

According to Eqs. 1 and 2, the MOE of fiber and parenchymatous ground tissue can be calculated by

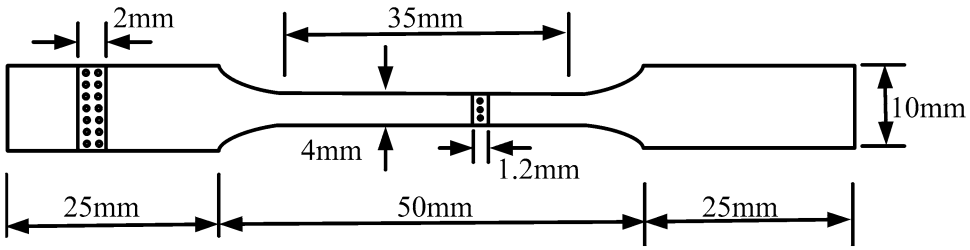

Fig. 1 Shape and dimension of the bamboo specimens for tensile test

analyzing the relationship between the MOE of bamboo specimen and the corresponding fiber volume fraction.

Materials and experimental methods

Experimental material and tension specimen

The moso bamboo (*Phyllostachys pubescens*) used in the experiment was 4 years old, and acquired from the Lingfeng hill (30°36′27.63 N, 119°38′29.54 E), Anji County, Zhejiang Province, China. The total height was about 11.5 m, and the diameter at breast height was 9–10 cm. Specimens were taken from internode sections, which were full meters (from 1 to 10 m) above the ground. The culm sections were longitudinally split into 100 mm (longitudinal) × 10 mm (tangential) strips after air-drying. Each strip was delaminated into four pieces. The distribution density of bamboo fiber increases from the inner to the outer part of the culm wall along the radial direction in the transverse section of moso bamboo. Therefore, bamboo is a typical functional gradient material. As the radial thickness of the specimen has the small size (1.2 mm), the specimen can be considered as a uniformly unidirectional fiber-reinforced bio-composite. To keep fiber alignment straight, each strip was delaminated into four pieces in the radius direction along the fiber direction after the culm sections were longitudinally split into strips. As the pieces are relatively short, fiber integrity has been maintained well in the pieces, and then polished the pieces very carefully to make sure most of the fiber keeps straight in the specimens. Thus, the final shape and the dimension of the specimens for tensile tests are shown in Fig. 1.

Measurement of mechanical properties of moso bamboo

Tensile tests on bamboo test specimens

Tensile tests were performed on an Instron model 5848 ultra-high precision materials testing machine. The equilibrium moisture content of the specimens was 9.7 %, the test room temperature was 25 °C, and the humidity was 19 %. The

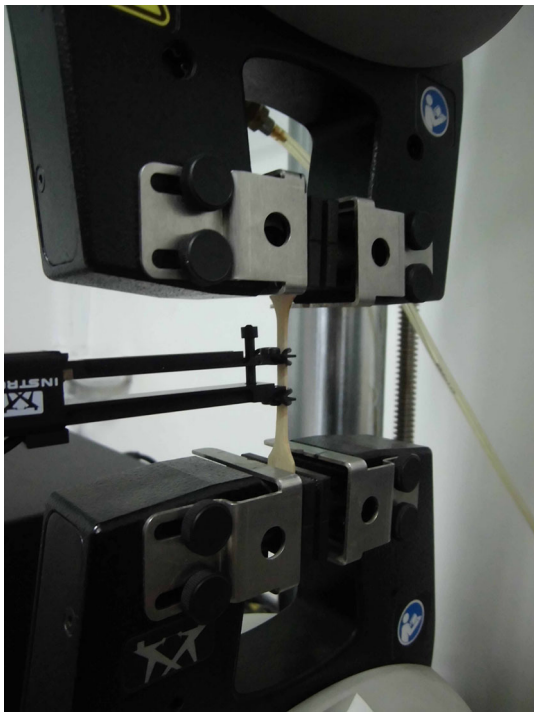

Fig. 2 Specimen mounted in the materials testing machine

specimens were placed on the testing machine with a displacement sensor installed on the effective experiment section of the specimen to obtain the elongation (Fig. 2). The specimens were loaded at a constant crosshead speed of 1 mm/min until tensile strain reaches 1 %. Figure 3 shows that four σ–ε curves are measured on bamboo blocks with different V_f values. The parts from the beginning of loading to the ending point were entirely linear. Thus, the MOE of each specimen can be calculated with the strain scope of 0.2–0.5 % according to its σ–ε curve.

Fiber volume fraction measurement

After the tensile tests, samples were taken near the fracture surface of the bamboo specimens to estimate the value of V_f by measuring A_f/A on transverse sections. After polishing until being smoothed, the transverse sections of the specimens were observed under a stereoscopic microscope to get the images of the sections. The values of A_f/A were then measured by Digimizer, which is an image analysis

software. An example of a series of treated images of the sample section from the outer to the inner part of a culm wall is shown in Fig. 4. The volume fractions of fiber were 42.39, 22.53, 14.98, and 11.11 %, respectively.

Mechanical properties of moso bamboo

Scatter diagram of the relationship between V_f and MOE was done linear fit, equation of linear regression and the corresponding trend line were obtained and shown in Fig. 5. The coefficient of determination R^2 is 0.9368, which indicates using equation of linear regression to describe the relationship of V_f and MOE is appropriate. When the MOE and fiber volume fraction were associated with each other, significant and positive linear relationships, were found between the MOE and V_f of the specimens, as shown in Fig. 5.

Based on the fitted linear equation between the MOE and V_f of the specimens,

$$E = 40.839\,V_f + 0.448 = 41.287\,V_f + 0.448\,(1 - V_f) \quad (3)$$

The MOE of fiber and parenchymatous ground tissue were estimated as $E_f = 41.287$ GPa and $E_p = 0.448$ GPa via Eq. 3. And the numerical values of V_f and MOE are similar to those in the Ref. [14], respectively, in which $E_f = 40.4$ GPa and $E_p = 0.22$ GPa. The difference between the values of E_p may be due to the type difference of moso bamboo. Thus, it can be seen that fiber is the main load-carrying part which determines the tensile properties of bamboo. Besides, the results support the hypothesis that bamboo is a unidirectional fiber-reinforced composite.

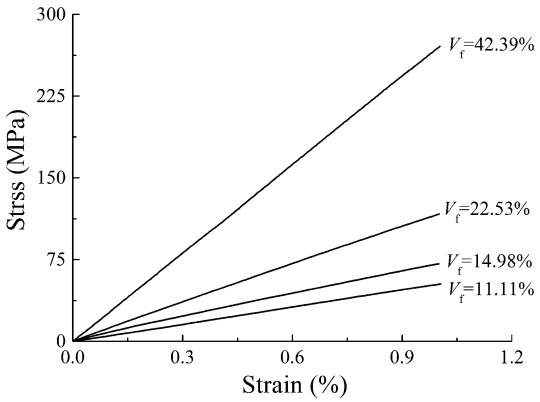

Fig. 3 Stress–strain curves of tensile tests on bamboo specimens with different fiber volume fractions

Finite-element analyses of bamboo

The hollow structure, as well as the gradient distribution of bamboo fiber is the embodiment of the superior bamboo construction. To validate this, numerical models were built based on the experimental data for comparative analysis.

The effect of hollow structure on behavior of bamboo structure

When the total amount of the material as well as the height of the structure is constant, the hollow structure has

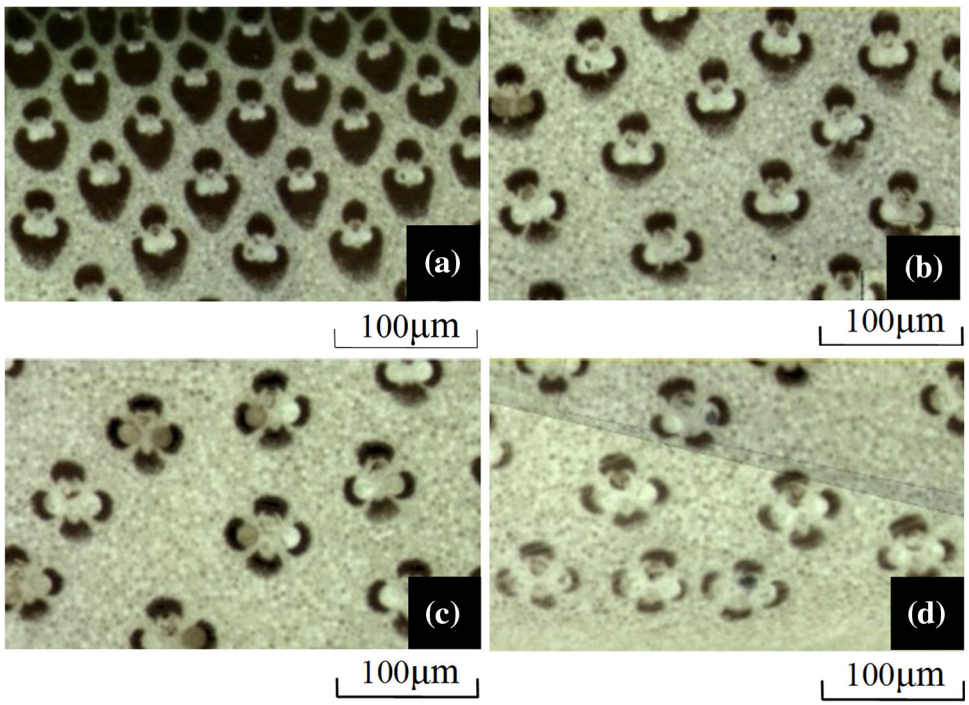

Fig. 4 Section images obtained from microscope. **a–d** Cross images of sections of the samples located along the radial direction from the outer to the inner part of a culm wall and the corresponding values of V_f were 42.39, 22.53, 14.98, and 11.11 %, respectively

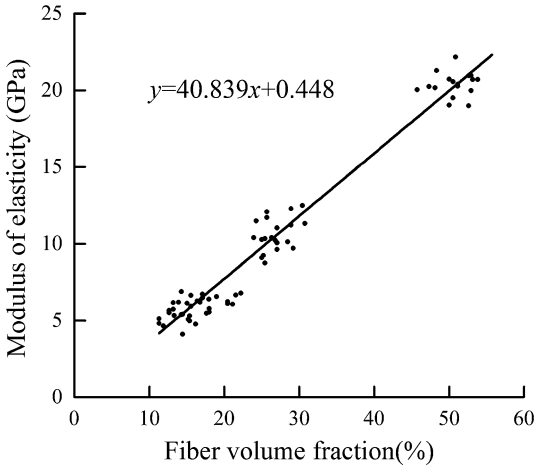

Fig. 5 Relationship between fiber volume fraction (V_f) and MOE of bamboo specimen

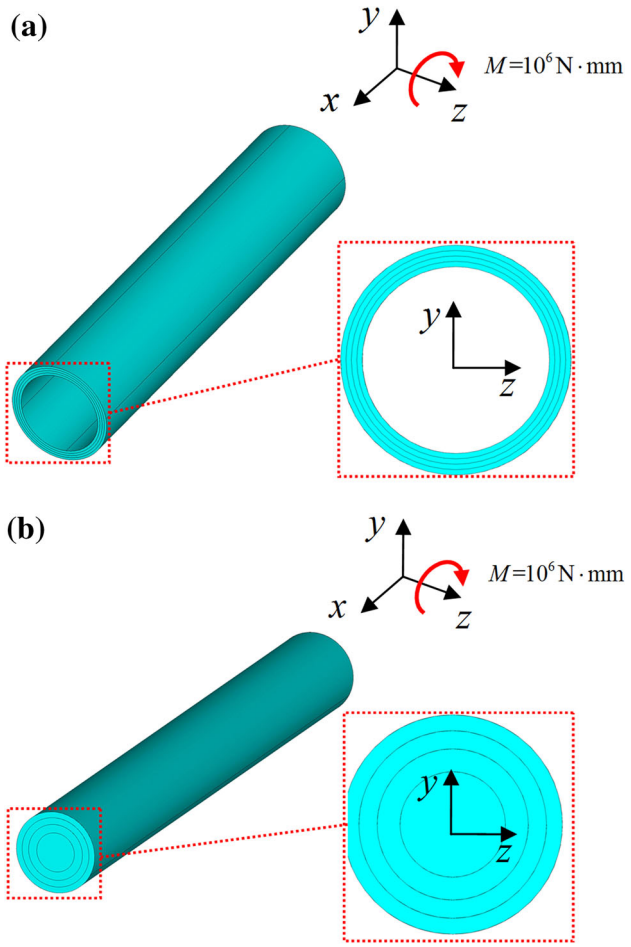

Fig. 6 The hollow model (**a**) and the solid model (**b**)

obvious advantages over solid structure in bearing loads. To validate the superiority of the hollow structure of bamboo, a numerical hollow model and a numerical solid model with equivalent volume of material were built to make comparative analysis on their mechanical behavior. The hollow model is a hollow tubular structure with a length of 500 mm, an outer radius of 52.83 mm, and an inside radius of 42.96 mm. The dimension data comes from the measured data of a section of moso bamboo. The solid model, which can be thought as wood which has a solid structure with graded elastic properties depended on microfibril angle in the cell wall, was built to emphasize the advantages of hollow reinforced tubular structures. The hollow model and solid model (Fig. 6) are divided into 4 layers along the radial direction, respectively, getting the axial MOE of each layer from the tensile results of bamboo specimens. Anisotropic materials were used in the two models. The mechanical properties of the material of each layer are the same except the axial MOE (E_x), which is shown in Tables 1, 2.

Table 1 The values of axial MOE of each layer (GPa)

1st layer (outermost layer)	2nd layer	3rd layer	4th layer
27.34	14.50	8.16	6.87

Table 2 Material mechanical properties of bamboo model

E_x (GPa)	E_y (GPa)	E_z (GPa)	G_{xy} (GPa)	G_{yz} (GPa)	G_{xz} (GPa)	$\mu_{xy} = \mu_{yz} = \mu_{xz}$
See Table 1	2.10	2.10	20.00	1.00	1.00	0.32

To simulate the actual situation of bamboo, the analysis model is constrained by a fixed end, and the other end is free. A bending moment of 10^6 N mm is loaded at the free end.

Since the hollow model and solid model are divided into 4 layers along the radial direction, respectively, the axial MOE E_{xi} and inertia moment I_{zi} of each layer are different from layer to layer. Thus, $M = \sum M_i$, and the bending moment M_i of each layer can be obtained by Eq. 4.

$$\frac{1}{\rho} = \frac{M_i}{E_{xi} I_{zi}} \tag{4}$$

The maximum axial stress appeared on the cross section in the middle position of each model can be calculated via Eq. 5, an equation for calculating the maximum stress of pure bending.

$$\sigma_{\max} = \frac{E_{xi} y_{\max}}{\rho} \tag{5}$$

The maximum displacement of each model can be acquired by using the unit load method. The displacement calculation equation is as Eq. 6.

$$\Delta = \int_0^l \frac{\overline{M} M_i}{E_{xi} I_{zi}}, \tag{6}$$

Table 3 The analytical and numerical solutions of hollow model and solid model

Model	Maximum displacement (mm)		Maximum axial stress on the middle cross section (MPa)	
	Analytical solution	Numerical solution	Analytical solution	Numerical solution
Hollow model	2.337	2.333	27.000	27.006
Solid model	9.374	9.414	63.047	63.407

where $\overline{M}$ is the bending moment caused by the unit load.

Thus, analytical and numerical solutions of the two models are solved, and the data of maximum deformation as well as maximum axial stress that appeared on the cross section in the middle position of each model are extracted from the solved results.

The analytical and numerical solutions of hollow model (Fig. 6a) and solid model (Fig. 6b) are shown in Table 3. As seen from the table, there is very small difference between the solutions of the analytical model and the numerical model. The maximum error between the two solutions is only 0.57 %.

For the purpose of comparing the analytical and numerical solutions of the maximum axial stress, the maximum axial stress that appeared on the cross section in the middle position of each model is extracted from the results, as is shown in Fig. 7a, b.

As we can see in Fig. 7, the analytical and numerical solutions of the maximum axial stress that appeared on the cross section in the middle position of each model agreed well with each other in every layer, but differ in the border between two layers; because the axial MOE of the analytical model suddenly changed in the border at the adjacent surface of two layers, the axial stress appeared step changed in the analytical model. While the axial stress in numerical model was the average of the axial stress at the junction of two layers.

By comparing the analytical solutions of the two models, we can notice that the maximum displacement of hollow model is only equal to 24.93 % of that of solid model, while the maximum axial stress in the middle position of hollow model is only 42.83 % of that of solid model. Accordingly, we can draw a conclusion that under the condition of using the same material, hollow structure of moso bamboo has clear and significant advantages over solid structure on the aspects of strength and stiffness.

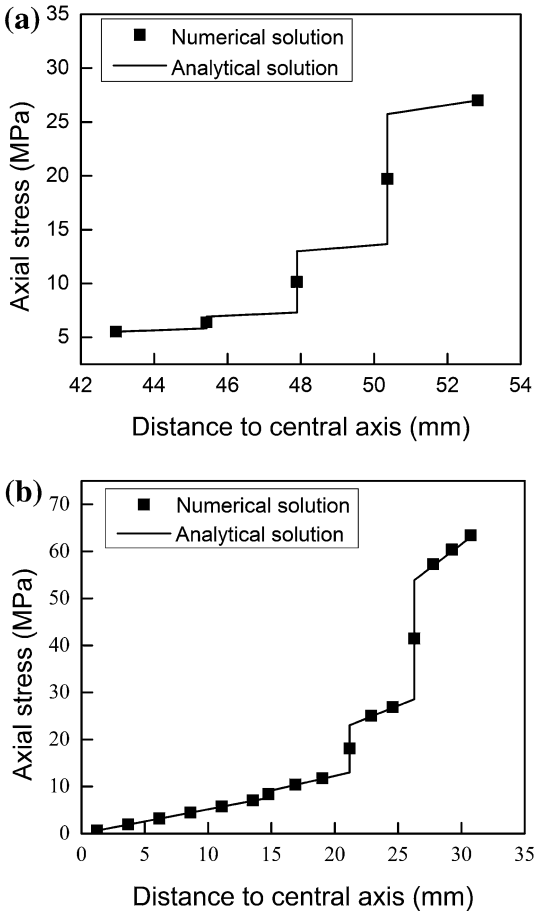

Fig. 7 Axial stress of solid model (**a**) and hollow model (**b**)

The effect of fiber gradient distribution on behavior of bamboo structure

Bamboo fiber volume fractions decrease along the radial direction from the outer to the inner part of a culm wall, making bamboo become a typical functionally graded material. For the purpose of analyzing the effects of fiber gradient distribution on behavior of bamboo structure, models, which are composed of fiber and parenchymatous ground tissue, were built based on different fiber distributions for comparative analysis.

By analyzing the shape and distribution rule of bamboo fiber on cross sections of natural bamboo (Fig. 8), squares and triangles with different sizes are arranged in a hierarchy to simulate the distribution of bamboo fiber, while materials among the fibers are set to be a parenchymatous tissue. In the Fig. 8a, the dark part, which can be fit into a square, represents that the shape of fiber can be simplified as square. The area of the fiber close to outer of bamboo is so small that we use triangle to simulate it. As to the distribution of bamboo fiber, the geometric centers of the

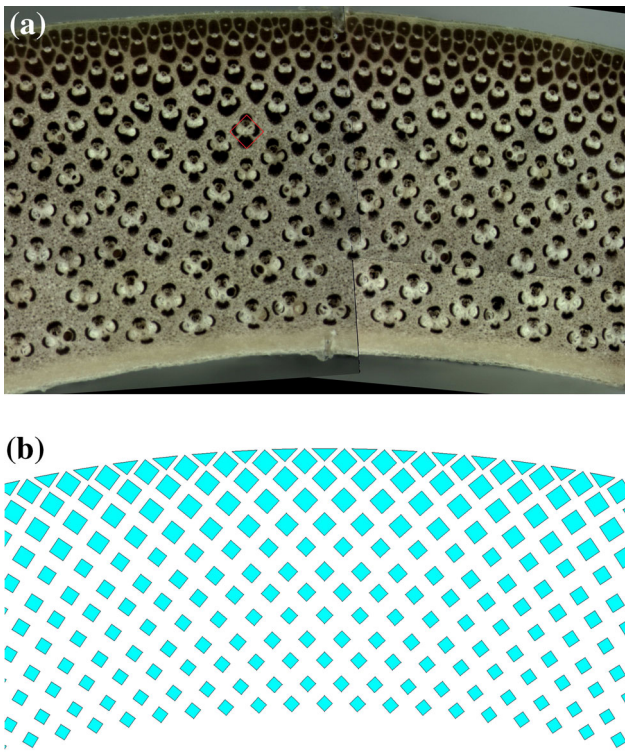

Fig. 8 Cross section of natural bamboo (**a**) and numerical model (**b**)

adjacent squares in circumferential direction are on the same circle, there is the same number of squares on the same circle, and we control the fiber percentage by adjusting the square area in the layers from outer to inner.

Three numerical models composed of fiber and parenchymatous ground tissue were built. The first model (Model I) is solid cylinder, which has the same material volume with the solid model as Fig. 6b (see Fig. 9a). Figure 9a shows the cross section of Model I, from which we can see fiber distributes evenly from outside to inside along the radial direction. The volume fraction of the fiber is 26.1 %, which comes from the measured data of moso bamboo. The second model (Model II) and the third model (Model III) are hollow cylinders whose shape and size are the same as the above-mentioned hollow model (see Fig. 6a). The difference between Model II and Model III is that the fiber of Model II distributes evenly from outside to inside along the radial direction (Fig. 9b) while the fiber has graded distribution in Model III (Fig. 9c).

To make the analysis effectively and comparatively of the three models, the cross section of each model was divided into 8 layers. Changing the fiber volume fraction of each layer simulates the uniform fiber distribution and the gradient fiber distribution of the three models. Figure 10 shows the fiber volume fraction of each layer of Model II (Fig. 10a) and Model III (Fig. 10b). By comparing the results of Model II and Model I, whether hollow structure

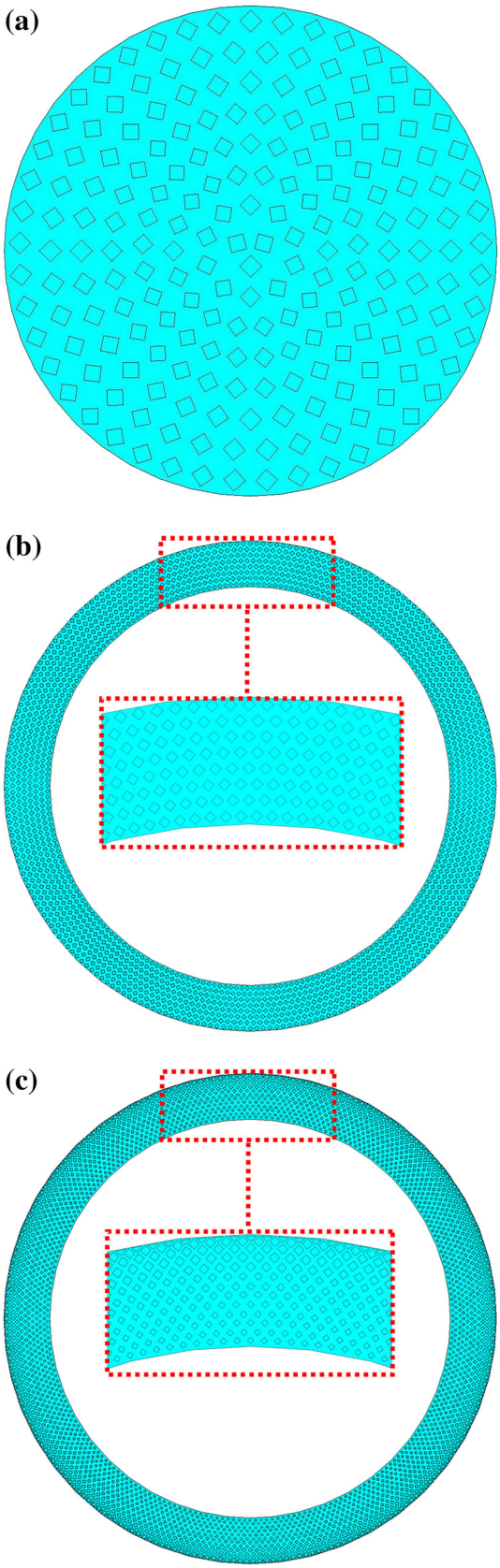

Fig. 9 Cross section of Model I (**a**), Model II (**b**) and Model III (**c**)

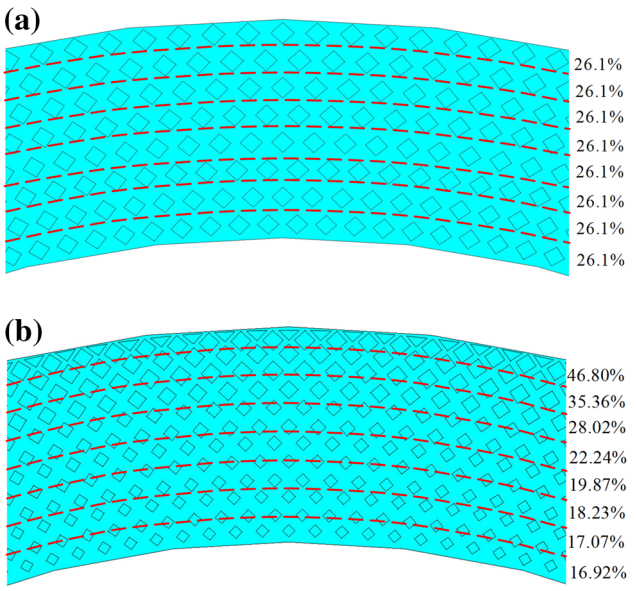

Fig. 10 Fiber volume fraction of each layer of Model II (**a**) and Model III (**b**)

Table 4 Maximum displacement and maximum axial stress

Model	Maximum displacement (mm)	Maximum axial stress (MPa)
Model I: solid model with uniform fiber distribution	12.249	172.830
Model II: hollow model with uniform fiber distribution	2.483	62.284
Model III: hollow model with gradient fiber distribution	2.177	54.915

has advantage over solid structure on strength and stiffness under the condition of using the same material can be studied. And comparing the results of Model II with those of Model III, we can investigate that whether the fiber gradient distribution of bamboo makes the mechanical performance excellent for the bamboo structure.

The three models were solved under the same loads and boundary conditions. The maximum displacement of the whole model as well as the maximum axial stress on the cross section in the middle position of the model is extracted from the solution, as is shown in Table 4.

By comparing the results of Model II and Model I, it can be seen that the maximum displacement of Model II is only 20.27 % of the maximum displacement of Model I, while the maximum axial stress in the middle position of the former is only 36.04 % of the latter. This illustrates that under the condition of using the same material, hollow structure has clear advantage over solid structure on strength and stiffness.

Similarly, by comparing the results of Model II and Model III, we can see that the maximum displacement of Model III is 12.32 %, which is less than that of Model II; the maximum axial stress in the middle position of the former is 11.83 %, which is less than that of the latter. It shows that the mechanical properties of bamboo structure were significantly improved because of the fiber gradient distribution.

As we can see via comparison, the maximum displacement of Model III is only 17.77 % of the maximum displacement of Model I, while the maximum axial stress in the middle position of the former is only 31.77 % of that of the latter. Accordingly, we can conclude that under the condition of using the same material, hollow structures as well as the fiber gradient distribution of bamboo make the mechanics performance excellent for the bamboo structure.

For the purpose of characterizing the utilization degrees of tensile strengths of fiber and parenchymatous ground tissue in the analytical model, the notion of strength capacity is introduced below. Taking fiber as an example, the strength capacity of fiber is the ratio of the difference between the tensile strength and the maximum axial stress to the tensile strength of fiber. The ratio can be calculated by Eq. 7.

$$\alpha_{\mathrm{f}} = \frac{\sigma_{\mathrm{fb}} - \sigma_{\mathrm{b}}}{\sigma_{\mathrm{fb}}} \times 100\ \%, \tag{7}$$

where σ_{f} is the maximum axial stress and σ_{fb} is the tensile strength of fiber. The tensile strength of fiber σ_{fb} is 587.786 MPa, while the tensile strength of parenchymatous ground tissue σ_{mb} is 13.494 MPa. The maximum axial stresses of fiber and parenchymatous tissue in the middle position of each model are extracted from the solution, and the strength capacities of fiber and parenchymatous tissue are calculated, as is shown in Table 5.

By comparing the strength capacities of fiber and parenchymatous ground tissue of Model III and Model I, we can see that strength capacities of fiber and parenchymatous tissue of the former model is 29.88 and 7.82 %, which are greater than those of the latter model, respectively. In other words, assuming the safety factors of fiber and parenchymatous ground tissue in Model I are 1, then the safety factors of fiber and parenchymatous ground tissue in Model II are 2.83 and 2.89, respectively. Further on, the safety factors of fiber and parenchymatous ground tissue in Model III are 3.23 and 3.30, respectively. In the perspective of comparing the strength capacities of fiber and parenchymatous ground tissue of each model, it can be seen that hollow structure as well as fiber gradient distribution of bamboo are the major reason why bamboo structure has excellent mechanics performance.

Table 5 The residual strengths of fiber and parenchymatous ground tissue

Model numbers	Maximum axial stress of fiber σ_f (MPa)	Residual strengths of fiber α_f (%)	Maximum axial stress of parenchymatous ground tissue σ_m (MPa)	Residual strengths of parenchymatous ground tissue α_m (%)
Model I	177.640	69.78	1.362	89.91
Model II	62.833	89.31	0.471	96.51
Model III	55.096	90.63	0.413	96.94

Conclusion

The mechanical properties of moso bamboo were measured and simulated. The main results show that:

(1) The maximum displacement of hollow model is only 24.93 % of the maximum displacement of solid model, while the maximum axial stress in the middle position of hollow model is only 42.83 %. It illustrates that under the condition of using the same material, hollow structure, such as bamboo, has a clear advantage over solid structure on strength and stiffness.

(2) Bamboo fiber volume fractions decrease along the radial direction from the outer to the inner part of a culm wall making bamboo become a typical functionally graded material. Three models composed of fiber and parenchymatous ground tissue were built based on different fiber distributions for comparative analysis. Assuming the safety factors of fiber and parenchymatous ground tissue in the solid model are 1, then the safety factors of fiber and parenchymatous ground tissue in the fiber evenly distributed hollow model are 2.83 and 2.89, respectively; furthermore, the safety factors of fiber and parenchymatous ground tissue in the fiber gradient distributed hollow model are 3.23 and 3.30, respectively. It can be seen obviously that the mechanical properties of bamboo structure are significantly improved by hollow structure and fiber gradient distribution.

Acknowledgments The authors gratefully acknowledge the financial support by the National Natural Science Foundation of China (Grant No. 11272020).

References

1. Ahmad M, Kamke FA (2005) Analysis of Calcutta bamboo for structural composite materials: physical and mechanical properties. Wood Sci Technol 39:448–459
2. Low IM, Che ZY, Latella BA, Sim KS (2006) Mechanical and fracture properties of bamboo. Key Eng Mater 312:15–20
3. Wang HK, Li WJ, Ren D, Yu ZX, Yu Y (2014) A two-variable model for predicting the effects of moisture content and density on compressive strength parallel to the grain for moso bamboo. J Wood Sci 60:362–366
4. Amada S, Untao S (2001) Fracture properties of bamboo. Compos Part B-Eng 32:451–459
5. Obataya E, Kitin P, Yamauchi H (2007) Bending characteristics of bamboo (*Phyllostachys pubescens*) with respect to its fiber-foam composite structure. Wood Sci Technol 41:385–400
6. Verma CS, Chariar VM, Purohit R (2012) Tensile strength analysis of bamboo and layered laminate bamboo composites. Int J Eng Res Appl 2:1253–1264
7. Yu Y, Wang HK, Lu F, Tian G, Lin J (2014) Bamboo fibers for composite applications: a mechanical and morphological investigation. J Mater Sci 49:2559–2566
8. Gutu T (2013) A study on the mechanical strength properties of bamboo to enhance its diversification on its utilization. Int J Innov Technol Explor Eng 2:314–319
9. Liu DG, Song JW, Anderson DP, Chang PR, Hua Y (2012) Bamboo fiber and its reinforced composites: structure and properties. Cellulose 19:1449–1480
10. Ghavami K, Rodrigues CS, Paciornik S (2003) Bamboo: functionally graded composite material. Asian J Civ Eng 4:1–10
11. Lo TY, Cui HZ, Leung HC (2004) The effect of fiber density on strength capacity of bamboo. Mater Lett 58:2595–2598
12. Ray AK, Mondal S, Das SK, Ramachandrarao P (2005) Bamboo—a functionally graded composite-correlation between microstructure and mechanical strength. J Mater Sci 40:5249–5253
13. Wang HK, Tian GL, Li WJ, Ren D, Zhang XX, Yu Y (2015) Sensitivity of bamboo fiber longitudinal tensile properties to moisture content variation under the fiber saturation point. J Wood Sci 61:262–269
14. Shao ZP, Fang CH, Huang SX, Tian GL (2010) Tensile properties of Moso bamboo (*Phyllostachys pubescens*) and its components with respect to its fiber-reinforced composite structure. Wood Sci Technol 44:655–666
15. Silva ECN, Walters MC, Paulino GH (2006) Modeling bamboo as a functionally graded material: lessons for the analysis of affordable materials. J Mater Sci 41:6991–7004
16. Tan T, Rahbar N, Allameh SM, Kwofie S, Dissmore D, Ghavami K, Soboyejo WO (2011) Mechanical properties of functionally graded hierarchical bamboo structures. Acta Biomater 7:3796–3803